

# On the galaxy–halo connection in the EAGLE simulation

Harry Desmond<sup>1,2\*</sup>, Yao-Yuan Mao<sup>3,4</sup>, Risa H. Wechsler<sup>1,2</sup>, Robert A. Crain<sup>5</sup>, and Joop Schaye<sup>6</sup>

<sup>1</sup>Kavli Institute for Particle Astrophysics and Cosmology, Physics Department, Stanford University, Stanford, CA 94305, USA

<sup>2</sup>SLAC National Accelerator Laboratory, Menlo Park, CA 94025, USA

<sup>3</sup>Department of Physics and Astronomy, University of Pittsburgh, Pittsburgh, PA 15260, USA

<sup>4</sup>Pittsburgh Particle Physics, Astrophysics, and Cosmology Center (PITT PACC), Pittsburgh, PA 15260, USA

<sup>5</sup>Astrophysics Research Institute, Liverpool John Moores University, 146 Brownlow Hill, Liverpool, L3 5RF, UK

<sup>6</sup>Leiden Observatory, Leiden University, P.O. Box 9513, 2300 RA Leiden, the Netherlands

3 July 2017

## ABSTRACT

Empirical models of galaxy formation require assumptions about the correlations between galaxy and halo properties. These may be calibrated against observations or inferred from physical models such as hydrodynamical simulations. In this *Letter*, we use the EAGLE simulation to investigate the correlation of galaxy size with halo properties. We motivate this analysis by noting that the common assumption of angular momentum partition between baryons and dark matter in rotationally supported galaxies overpredicts both the spread in the stellar mass–size relation and the anticorrelation of size and velocity residuals, indicating a problem with the galaxy–halo connection it implies. We find the EAGLE galaxy population to perform significantly better on both statistics, and trace this success to the weakness of the correlations of galaxy size with halo mass, concentration and spin at fixed stellar mass. Using these correlations in empirical models will enable fine-grained aspects of galaxy scalings to be matched.

**Key words:** galaxies: formation – galaxies: fundamental parameters – galaxies: haloes – galaxies: kinematics and dynamics – galaxies: statistics – dark matter

## 1 INTRODUCTION

Accurate semi-analytic and empirical modelling of galaxy formation is challenging, in part because the correlations of key galaxy and halo variables remain unknown. Observational manifestations of these correlations include galaxy scaling relations, and through detailed investigations of these relations we may hope to build knowledge of the galaxy–halo connection.

Over the past decades, two models which have proven useful for capturing aspects of the galaxy–halo connection are subhalo abundance matching (SHAM; Kravtsov et al. 2004; Behroozi et al. 2010), and the angular momentum model of Mo, Mao & White (1998, hereafter MMW). SHAM asserts a nearly monotonic relationship between stellar mass and a halo proxy, establishing the dependence of galaxy mass on halo mass and concentration required to reproduce galaxy clustering (e.g. Conroy, Wechsler & Kravtsov 2006; Reddick et al. 2013). The MMW model sets galaxy and halo specific angular momentum proportional and assumes galaxies’ velocities to be entirely rotational, making galaxy size a function of galaxy mass and halo mass, concentration and spin. This agrees well with observed average galaxy sizes over a wide range of mass (Kravtsov 2013; Desmond & Wechsler 2015, hereafter DW15).

Despite these successes, however, the conjunction of these models (hereafter “SHAM+MMW”) is known to make incorrect predictions for two properties of the galaxy population. The first is the scatter  $s_{\text{MSR}}$  in the stellar mass–size relation (MSR; de Jong & Lacey 2000; Gnedin et al. 2007). SHAM+MMW sets galaxy size proportional to halo spin,  $\lambda$ , and hence requires the scatter in size at fixed mass to be at least as large as that in  $\lambda$ . In fact, these scatters are  $\sim 0.2$  dex and  $\sim 0.25$  dex in observed galaxies and simulations respectively (DW15). The second is the correlation of residuals of the mass–size and mass–velocity relations ( $\rho_{\Delta R-\Delta V}$ ), which is negligible in observations but predicted to be negative (McGaugh 2005; Dutton et al. 2007; DW15). These discrepancies indicate that the galaxy–halo correlations on which  $s_{\text{MSR}}$  and  $\rho_{\Delta R-\Delta V}$  depend are inadequately captured by the model.

This issue is relevant also for semi-analytic models. Many such models set galaxy size proportional to halo virial radius (e.g. Somerville et al. 2008; Croton et al. 2006; Lu et al. 2011), sometimes with a single value for all halo spins. Others that use additional physical assumptions find important correlations of size with variables beyond halo mass and spin, but neglect the scatter in sizes (e.g. Lu, Mo & Wechsler 2015). The empirical identification of the aspects of the galaxy–halo connection responsible for realistic size distributions – and correlations with velocity – will be of use in constraining such models and guiding the choice of inputs.

\* E-mail: harryd2@stanford.edu

The failure of SHAM+MMW may be due either to inaccuracies in the properties of the halo populations on which the models were based (e.g. their neglect of baryonic physics), or incorrect prediction of the models themselves for the galaxy–halo connection. To resolve this dilemma, we turn in this *Letter* to hydrodynamical simulations, which enable the prediction of galaxy properties without prior assumptions on galaxy–halo correlations. In particular, we investigate  $s_{\text{MSR}}$  and  $\rho_{\Delta R-\Delta V}$  in the EAGLE simulation (Schaye et al. 2015; Crain et al. 2015),<sup>1</sup> which has previously been shown to match the galaxy size distribution as well as many other aspects of galaxy phenomenology (Furlong et al. 2015). Sales et al. (2009) and Stevens et al. (2016) showed that the MMW model fails to match the output of the EAGLE simulation and its ancestor OWLS. Zavala et al. (2016) found the angular momentum of stars to correlate with that of the inner halo in EAGLE, and Sales et al. (2012) reported weak correlation of galaxy properties with halo spin in the related GIMIC simulation. This is in contrast with other simulations in which halo spin correlates more strongly with galaxy spin and morphology, especially at low mass (e.g. Teklu et al. 2015; Rodriguez-Gomez et al. 2017). Finally, Ferrero et al. (2016) studied the EAGLE Tully–Fisher and mass–size relations.

The structure of this paper is as follows. In Section 2 we describe the EAGLE simulation and our methods to measure and explore the origin of  $s_{\text{MSR}}$  and  $\rho_{\Delta R-\Delta V}$ . In Section 3.1 we show that both  $s_{\text{MSR}}$  and  $\rho_{\Delta R-\Delta V}$  are significantly nearer their observed values in EAGLE than in the SHAM+MMW model, and close to the predictions of SHAM alone. We show the success of EAGLE over SHAM+MMW to be due not to differences in underlying halo properties caused by baryons (Section 3.2), but rather to the correlations of halo variables with galaxy size (Section 3.3). In EAGLE, the sizes of low-redshift galaxies are only weakly correlated at fixed stellar mass with the mass, concentration and spin of their haloes, violating the assumption of angular momentum partition. Section 4 discusses the broader implications of these results, and summarises.

## 2 SIMULATIONS AND METHODS

### 2.1 The EAGLE simulation

EAGLE is a recently completed set of cosmological hydrodynamical simulations, run with a modified version of GADGET-3 (Springel 2005) and including hydrodynamics, radiative cooling, star formation, stellar feedback and black hole dynamics. The subgrid models were calibrated against the present-day stellar mass function and the normalisation of the mass–size relation. The simulations used a flat  $\Lambda$ CDM cosmology with  $\Omega_{\text{m}} = 0.307$ ,  $\Omega_{\text{b}} = 0.04825$ ,  $h = 0.6777$ ,  $\sigma_8 = 0.8288$  and  $n_s = 0.9611$ . We analyse the  $z = 0$  snapshot of simulation Ref-L100N1504, which tracks  $1504^3$  dark matter and gas particles from  $z = 127$  to the present day in a box with comoving side length 100 Mpc, in addition to the corresponding dark matter only (DMO) run in which baryonic effects were switched off. We refer the reader to Schaye et al. (2015) and Crain et al. (2015) for further information about the simulation.

### 2.2 Finding and matching haloes

To enable direct comparison with the results of DW15, we perform halo finding on both the DMO and hydrodynamical (hereafter “hydro”) runs of the EAGLE simulation using ROCKSTAR (Behroozi

et al. 2013). We define spin as  $\lambda \equiv J|E|^{1/2}G^{-1}M^{-5/2}$ , where  $J$  is a halo’s angular momentum and  $E$  its total energy (Peebles 1969), and calculate concentration ( $c$ ) using  $r_{s,\text{klypin}}$  (derived from  $V_{\text{max}}/V_{\text{vir}}$ ; Klypin et al. 2001) rather than fitting an NFW profile. We include only dark matter when calculating  $c$  and  $\lambda$ . We multiply the DMO haloes’ virial masses by  $1 - \Omega_{\text{b}}/\Omega_{\text{m}}$  to compare to the hydro haloes, where again we include dark matter only ( $M_{\text{DM}}$ ).

Next, we match the DMO ROCKSTAR catalogue to both the hydro ROCKSTAR catalogue and the SUBFIND catalogue (Springel et al. 2001; Dolag et al. 2009) made by the EAGLE pipeline, as follows. Both halo finders produce a list of particles associated with each halo that they identify. Since the two runs share the same dark matter particle IDs, we can match the haloes by finding common particles. In practice, given a halo in the DMO run (halo A), we first find the halo (halo B) in the hydro run that contains the most particles of halo A. If halo A also contains the most particles of halo B, we identify a “match” between them. Since the SUBFIND catalogue of the hydro run also provides the connection between the haloes and galaxies, this method establishes a link between the haloes in the DMO and hydro ROCKSTAR catalogues, and the galaxies in the SUBFIND catalogue. The fraction of haloes in the hydro run hosting galaxies with  $M_* > 10^9 M_{\odot}$  that are matched by our procedure is 91 per cent; these haloes are not significantly biased in  $M_{\text{DM}}$ ,  $c$  or  $\lambda$ .

### 2.3 Data, models and statistics

We compare our models with the observations of Pizagno et al. (2007, hereafter P07) for compatibility with DW15. Although larger samples with well-measured sizes now exist (e.g. Huang et al. 2017; Somerville et al. 2017), they produce similar MSRs. P07 require an apparent axis ratio  $b/a \leq 0.6$  and usable  $H\alpha$  rotation curve, which they find not to significantly bias the admitted galaxy population in colour or concentration. We therefore do not make a morphology cut on the EAGLE galaxies in our fiducial analysis, although we have checked that our results change at no more than the  $\sim 1\sigma$  level – and our qualitative conclusions remain unchanged – when only including galaxies with a substantial fraction of their kinetic energy in ordered corotation ( $\kappa_{\text{co}} \geq 0.4$ ; Correa et al. 2017). We compare the EAGLE results with two semi-empirical models, denoted “SHAM” and “SHAM+MMW” as in Section 1.

For both data and models, we take  $s_{\text{MSR}}$  to be the Gaussian scatter in radius of the best-fitting power-law relation<sup>2</sup> between stellar mass ( $M_*$ ) and half-mass radius ( $R_{\text{eff}}$ ; measured for stars in a 30 kpc aperture), over the range  $9 < \log(M_*/M_{\odot}) < 11.5$ . We have verified that restricting to  $\log(M_*/M_{\odot}) > 10$  does not affect our conclusions. We measure  $\rho_{\Delta R-\Delta V}$  as the Spearman rank correlation coefficient of the  $\Delta R_{\text{eff}} - \Delta V_{\text{max}}$  relation, where  $\Delta x$  denotes the residual of quantity  $\log(x)$  after subtracting the value expected at that  $M_*$  given a power-law fit to the  $\log(M_*) - \log(x)$  relation,  $f_x(M_*)$ :

$$\Delta x \equiv \log(x) - f_x(M_*). \quad (1)$$

We quantify the dependence of  $R_{\text{eff}}$  on halo variables with the Spearman correlation coefficients  $\rho_{\Delta R-\Delta X}$ , where  $X \in \{M_{\text{DM}}, c, \lambda\}$ . We record in Table 1 the median and  $1\sigma$  spread of the statistics over 100 Monte Carlo mock data sets of galaxies with  $M_*$  values within 0.01 dex of those of the observational sample (see Section 3.1).

<sup>2</sup> Note that the use of a power law in this definition means that  $s_{\text{MSR}}$  is increased by curvature in the MSR; thus  $s_{\text{MSR}}$  for the EAGLE relation (see Fig. 1a) may be considered an upper bound on the “true” intrinsic scatter.

<sup>1</sup> <http://eagle.strw.leidenuniv.nl>

	P07	EAGLE	SHAM	SHAM+MMW
$s_{\text{MSR}}$	0.18	$0.15 \pm 0.01$	<i>0.18</i>	$0.39 \pm 0.03$
$\rho_{\Delta R-\Delta V}$	-0.07	$-0.13 \pm 0.07$	$-0.22 \pm 0.04$	$-0.56 \pm 0.05$
$\rho_{\Delta R-\Delta M_{\text{DM}}}$	–	$0.18 \pm 0.07$	0	$0.75 \pm 0.04$
$\rho_{\Delta R-\Delta c}$	–	$-0.19 \pm 0.07$	0	$-0.76 \pm 0.04$
$\rho_{\Delta R-\Delta \lambda}$	–	$0.17 \pm 0.08$	0	$0.80 \pm 0.04$

**Table 1.** Comparison of statistics of the galaxy–halo connection in observations (P07), the EAGLE simulation, an abundance matching model with sizes chosen to match the stellar mass–size relation by construction (“SHAM”), and an analogous model with sizes set by angular momentum partition (“SHAM+MMW”; Desmond & Wechsler 2015).  $s_{\text{MSR}}$  is the scatter in size of the stellar mass–size relation,  $\rho$  denotes Spearman rank correlation coefficient, and  $\Delta$  is defined in Eq. 1. Entries in italics are by construction. The SHAM+MMW model overpredicts both  $s_{\text{MSR}}$  and  $|\rho_{\Delta R-\Delta V}|$  due to the strong correlations it implies between  $R_{\text{eff}}$  and  $M_{\text{DM}}$ ,  $c$  and  $\lambda$  at fixed  $M_*$ . The EAGLE galaxy–halo connection, in which these variables are only weakly correlated, performs significantly better on both statistics.

## 3 RESULTS

### 3.1 The EAGLE mass–size and $\Delta R - \Delta V$ relations

Figure 1a shows the MSR of the EAGLE galaxies, and Figure 1b the correlation of their size and velocity residuals. That both EAGLE relations are in approximate agreement with the P07 observations is verified quantitatively in the first two rows of Table 1, which list the  $s_{\text{MSR}}$  and  $\rho_{\Delta R-\Delta V}$  values.

The 3<sup>rd</sup> and 4<sup>th</sup> columns of Table 1 show analogous results for two alternative models. In “SHAM,”  $M_*$  is set by SHAM using the  $V_{\text{peak}}$  proxy and 0.2 dex scatter (Reddick et al. 2013; varying the SHAM parameters within the bounds set by clustering has a negligible effect on our results), and galaxy sizes are chosen randomly from a normal distribution at given  $M_*$  to match the P07 MSR by construction. In “SHAM+MMW,” sizes are set by the MMW model after SHAM has been performed, using the procedure and best-fitting parameter values of DW15.

As mentioned in Section 1 (and discussed in detail in DW15), the SHAM+MMW model compares poorly with observations in both  $s_{\text{MSR}}$  and  $\rho_{\Delta R-\Delta V}$ . This appears to be in conflict with Somerville et al. (2017), who claim the model generates an  $s_{\text{MSR}}$  in agreement with that of a compilation of GAMA and CANDELS data. However, they include only the contribution to  $s_{\text{MSR}}$  from scatter in  $\lambda$  ( $\sim 0.25$  dex) and neglect the contributions from scatter in  $M_{\text{DM}}$  and  $c$  at fixed  $M_*$ .  $\rho_{\Delta R-\Delta V}$  has contributions both from baryonic mass (higher surface density means larger rotation velocity), and from the dark matter, since in the MMW model more concentrated haloes, which generate larger rotation velocities, host smaller galaxies at fixed angular momentum. The SHAM model, which includes only the first contribution, predicts a  $\Delta R - \Delta V$  anticorrelation that is weaker but still stronger than the data’s. It is important to note, however, that these models assume negligible velocity dispersion  $\sigma$ . An decrease of  $\sigma/V_{\text{rot}}$  with  $\lambda$  – as produced in some hydrodynamical simulations (e.g. Rodriguez-Gomez et al. 2017) – could reduce the predicted  $|\rho_{\Delta R-\Delta V}|$  and  $s_{\text{MSR}}$ . Only with the assumption that  $\sigma/V_{\text{rot}}$  does not vary systematically with  $\lambda$  does the MMW model follow uniquely from proportionality of galaxy and halo specific angular momentum.

We now investigate the origin of the difference between the EAGLE and SHAM+MMW results.

### 3.2 Comparison of the haloes in the DMO and hydrodynamical runs of the EAGLE simulation

A possible reason for the apparent failure of the SHAM+MMW model is its application in DW15 to haloes from an N-body simulation in which baryonic effects were neglected. In Figure 2 we show the fractional differences in  $M_{\text{DM}}$ ,  $c$  and  $\lambda$  of all matched haloes in the EAGLE DMO and hydro runs, and compare in the insets their overall distributions. We find the haloes to be a few per cent less massive on average in the hydro run, and their  $c$  and  $\lambda$  values to be similar. (Schaller et al. 2015 reported larger differences in halo mass because they included baryons as well as dark matter in the mass definition.) The spin distribution is slightly wider in the hydro run, which goes in the wrong direction to account for the lower  $s_{\text{MSR}}$  in EAGLE than in the SHAM+MMW model.

In Figure 3 we compare the correlations of  $\lambda$  with  $M_{\text{DM}}$  and  $c$  in the two runs, finding them to be very similar. If spin was more positively correlated with  $M_{\text{DM}}$  or  $c$  with baryonic effects included, then the corresponding increase in rotational velocity caused by dark matter for larger galaxies would compensate for the reduction in the rotation velocity caused by baryons, which could allow the SHAM+MMW model to agree with the measured  $\rho_{\Delta R-\Delta V}$ . That we do not find such an increased correlation leads us to conclude that the differences between the EAGLE and SHAM+MMW models in their predictions for  $s_{\text{MSR}}$  and  $\rho_{\Delta R-\Delta V}$  arise not from underlying dark matter halo structure, but rather from differences in the correlations of galaxy and halo variables. It is to these that we now turn.

### 3.3 The galaxy–halo connection

Rows 3-5 of Table 1 record the Spearman rank coefficients of the correlations between size residual ( $\Delta R_{\text{eff}}$ ) and  $M_{\text{DM}}$ ,  $c$  and  $\lambda$  residual in the EAGLE, SHAM, and SHAM+MMW models. As halo properties cannot be observed, there are no corresponding entries in the first column. By construction, the SHAM model does not correlate galaxy size with any halo property at fixed stellar mass. As described in Section 1, however, the SHAM+MMW model implies a strong correlation of  $\Delta R_{\text{eff}}$  with  $\Delta \lambda$  and a strong anticorrelation with  $\Delta c$ , and the latter in particular is responsible for the strongly negative value of  $\rho_{\Delta R-\Delta V}$ . In the EAGLE simulation, galaxy size correlates only weakly with each halo variable, with the result that the predicted  $\rho_{\Delta R-\Delta V}$  is similar to the SHAM case. In addition, this prevents  $s_{\text{MSR}}$  from receiving the full contributions from the scatter in halo variables at fixed  $M_*$ , allowing it to remain below the P07 value. These correlations are shown explicitly in Figure 4.

## 4 DISCUSSION AND CONCLUSIONS

While the principle component of the galaxy–halo connection – the relation between galaxy mass and halo mass and concentration – is becoming well constrained by abundance matching studies, secondary components, such as the dependence of galaxy size on halo properties, remain uncertain. A leading model for galaxy size (Mo et al. 1998; MMW) assumes  $\sigma = 0$  and proportionality of galaxy and halo specific angular momenta, making galaxy size a specific function of stellar mass and halo mass, concentration and spin. Despite success in matching the normalisation of the stellar mass–size relation when combined with SHAM, this model overpredicts both the spread in sizes ( $s_{\text{MSR}}$ ) and the strength of the correlation of size and velocity residuals ( $\rho_{\Delta R-\Delta V}$ ). This indicates a problem with the galaxy–halo connection it implies.

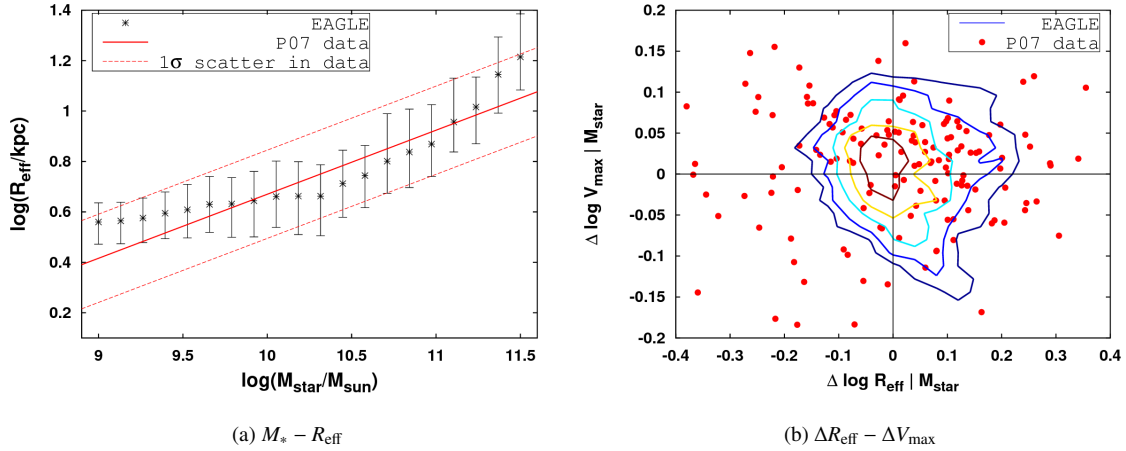


**Figure 1.** The  $M_* - R_{\text{eff}}$  relation and correlation of  $R_{\text{eff}}$  and  $V_{\text{max}}$  residuals in the EAGLE simulation, compared to the observations of Pizagno et al. (2007). As in DW15, stellar masses for the latter were taken from the NASA Sloan Atlas. The red lines in the left panel show the best-fitting power-law to the data, and its scatter. In this plot and those that follow, points indicate medians and error bars 16<sup>th</sup> and 84<sup>th</sup> percentiles. We stack the 100 mock data sets (Section 2.3) to make contour plots, and the levels enclose 90, 80, 60, 40 and 20 per cent of galaxies. The spread in the sizes of EAGLE galaxies is as low as is observed, and they correctly exhibit no significant  $\Delta R_{\text{eff}} - \Delta V_{\text{max}}$  correlation. In Fig. 1b, the observations have  $\rho_{\Delta R - \Delta V} = -0.07$ , and the EAGLE galaxies have  $\rho_{\Delta R - \Delta V} = -0.13$ .

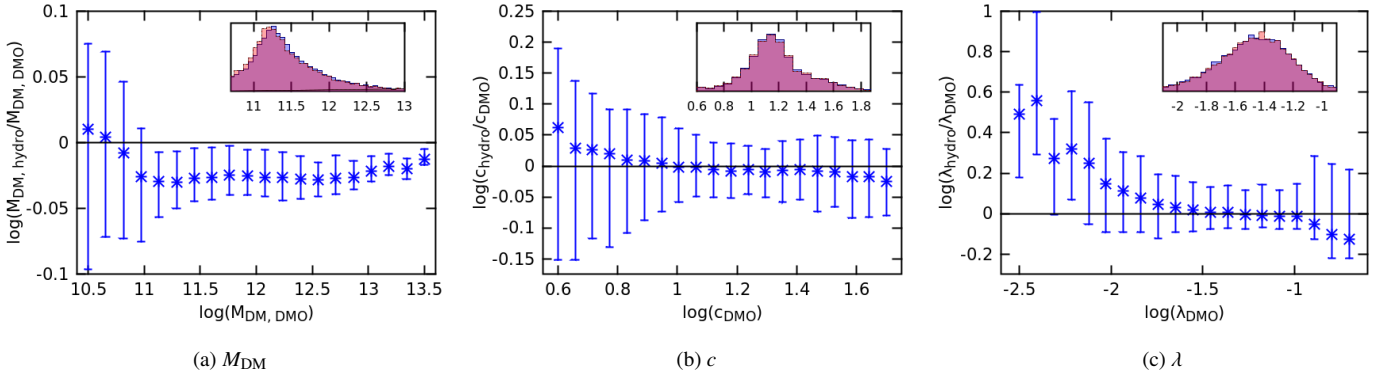


**Figure 2.** The differences in  $M_{\text{DM}}$ ,  $c$  and  $\lambda$  between all  $M_* > 10^9 M_{\odot}$  haloes in the hydro runs of the EAGLE simulation and their counterparts in the DMO run, as a function of the DMO variable. The insets compare the overall distributions (hydro in red and DMO in blue). With baryonic effects included,  $M_{\text{DM}}$  is reduced by a few per cent on average (the catalogue is incomplete for  $M_{\text{DM}} \lesssim 10^{11} M_{\odot}$ ), and  $\lambda$  increased slightly at low values.  $c$  is largely unaffected.

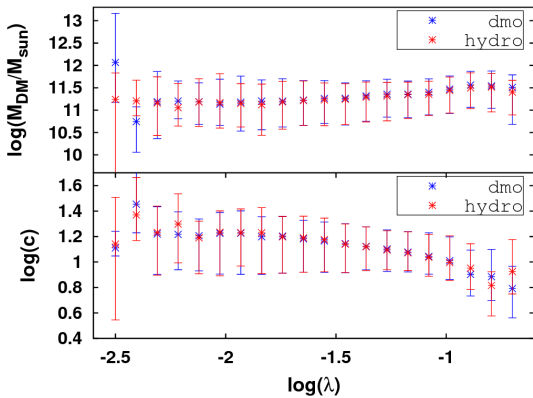


**Figure 3.**  $\lambda$  correlates in the same way with both  $M_{\text{DM}}$  and  $c$  in the DMO and hydro runs of EAGLE. Together with Fig. 2, this shows that the difference between the EAGLE and SHAM+MMW models in their predictions for  $s_{\text{MSR}}$  and  $\rho_{\Delta R - \Delta V}$  are not due to changes to the haloes caused by baryons. They must therefore be due to different galaxy–halo correlations.

In this *Letter*, we investigated this discrepancy in the context of the EAGLE hydrodynamical simulation. We found the galaxy population in this simulation to exhibit near-agreement with measurements of both  $s_{\text{MSR}}$  and  $\rho_{\Delta R - \Delta V}$ . We showed that this difference with the SHAM+MMW prediction is due not to modifications to the haloes themselves by baryons, but rather to the weakness of the correlations of galaxy size with  $M_{\text{DM}}$ ,  $c$  and  $\lambda$ . While the MMW model strongly correlates  $R_{\text{eff}}$  with  $M_{\text{DM}}$  ( $\rho = 0.75$ ),  $c$  ( $\rho = -0.76$ ) and  $\lambda$  ( $\rho = 0.80$ ) at fixed  $M_*$ , the Spearman rank coefficients for the corresponding EAGLE correlations are only 0.18,  $-0.19$  and 0.17, respectively. These values are consistent with 0 within  $3\sigma$ .

Our results have implications for both galaxy formation theory and semi-analytic and empirical modelling. On one hand, the breakdown of the MMW model requires explanation. Galaxy properties may become weakly correlated with halo spin due to stochastic transfer of angular momentum between baryons and dark matter, or a significant loss or redistribution through feedback or cooling processes (Brook et al. 2011; Zjupa & Springel 2016). On the other hand, the EAGLE galaxy–halo correlations may be used to inform



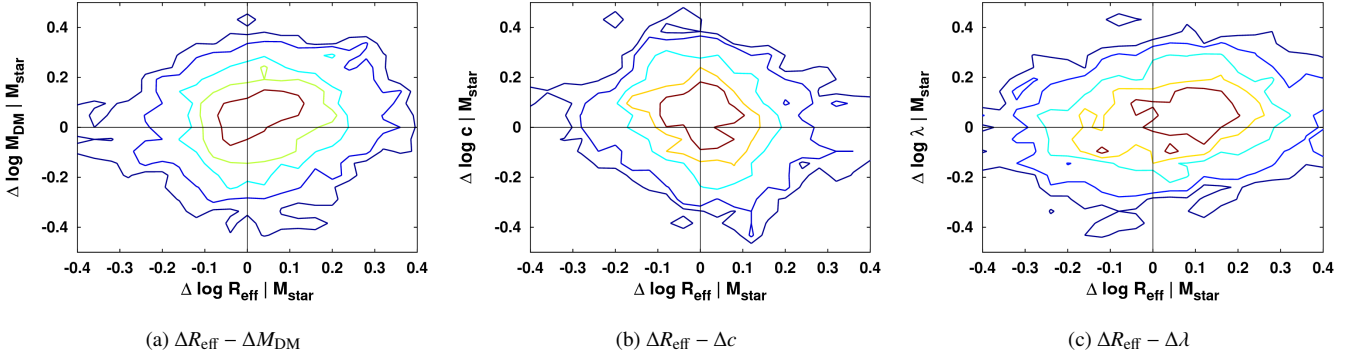


**Figure 4.** The correlation of residuals of the stellar mass–size relation with dark matter mass, concentration and spin residuals in the hydro run of the EAGLE simulation. Haloes were randomly selected from the catalogue to reproduce the stellar mass distribution of the P07 sample (see Section 2.3). In contrast to the SHAM+MMW model, EAGLE predicts these correlations to be weak, which accounts for the better agreement of the predicted  $s_{\text{MSR}}$  and  $\rho_{\Delta R-\Delta V}$  values with the observations. The Spearman rank correlation coefficients of these relations are 0.18,  $-0.19$  and 0.17, respectively (see Table 1).

empirical models where galaxy sizes are added by hand. To match  $s_{\text{MSR}}$  and  $\rho_{\Delta R-\Delta V}$ , at least in a SHAM framework,  $R_{\text{eff}}$  should correlate at most weakly with  $M_{\text{DM}}$ ,  $c$  and  $\lambda$  at fixed  $M_*$ . This is tacitly assumed by several existing models (e.g. Dutton et al. 2011, 2013; Desmond & Wechsler 2016), and implied also by aspects of the mass discrepancy–acceleration relation (Desmond 2017). We suggest such correlations be used by default from now on. Finally, our results facilitate the testing of galaxy formation theories: if a theory’s effective galaxy–halo connection exhibits correlations compatible with those of EAGLE, its success in matching the fine-grained statistics that we investigate here is assured.

## ACKNOWLEDGEMENTS

We thank Simon Foreman, Yu Lu, and Matthieu Schaller for comments on the manuscript, and Matthieu Schaller for guidance with the EAGLE data. This work used the DiRAC Data Centric system at Durham University, operated by the Institute for Computational Cosmology on behalf of the STFC DiRAC HPC Facility (www.dirac.ac.uk). This equipment was funded by a BIS National E-infrastructure capital grant ST/K00042X/1, STFC capital grant ST/K00087X/1, DiRAC Operations grant ST/K003267/1 and Durham University. DiRAC is part of the National E-Infrastructure. HD received support from the U.S. Department of Energy, contract number DE-AC02-76SF00515. This work was supported by the Netherlands Organisation for Scientific Research (NWO), through VICI grant 639.043.409, and the European Research Council under the European Union’s Seventh Framework Programme (FP7/2007-2013) / ERC Grant agreement 278594-GasAroundGalaxies. RAC is a Royal Society University Research Fellow.

## REFERENCES

Behroozi P. S., Conroy C., Wechsler R. H., 2010, *ApJ*, 717, 379  
 Behroozi, P. S., Wechsler, R. H., & Wu, H.-Y. 2013, *ApJ*, 762, 109  
 Brook C. B. et al., 2011, *MNRAS*, 415, 1051  
 de Jong R. S., Lacey C., 2000, *ApJ*, 545, 781  
 Conroy C., Wechsler R. H., Kravtsov A. V., 2006, *ApJ*, 647, 201  
 Correa C. A., Schaye J., Clauwens B., Bower R. G., Crain R. A., Schaller M., Theuns T., Thob A. C. R., 2017, preprint (arXiv:1704.06283)  
 Crain R. A. et al., 2015, *MNRAS*, 450, 1937  
 Croton D. J. et al., 2006, *MNRAS*, 365, 11

Desmond H., Wechsler R. H., 2015, *MNRAS*, 454, 322  
 Desmond H., Wechsler R. H., 2017, *MNRAS*, 465, 820  
 Desmond H., 2017, *MNRAS*, 464, 4160  
 Dolag K., Borgani S., Murante G., Springel V., 2009, *MNRAS*, 399, 497  
 Dutton A. A., van den Bosch F. C., Dekel A., Courteau S., 2007, *ApJ*, 654, 27  
 Dutton A. A. et al., 2011, *MNRAS*, 416, 322  
 Dutton A. A., Macciò A. V., Mendel J. T., Simard L., 2013, *MNRAS*, 432, 2496  
 Ferrero I. et al., 2016, preprint (arXiv:1607.03100)  
 Furlong M. et al., 2016, preprint (arXiv:1510.05645)  
 Gnedin O. Y., Weinberg D. H., Pizagno J., Prada F., Rix H.-W., 2007, *ApJ*, 671, 1115  
 Huang et al., 2017, *ApJ*, 838, 6  
 Klypin, A., Kravtsov, A. V., Bullock, J. S., & Primack, J. R. 2001, *ApJ*, 554, 903  
 Kravtsov A. V., 2013, *ApJL*, 764, L31  
 Kravtsov A. V., Berlind A. A., Wechsler R. H., Klypin A. A., Gottlober S., Allgood B., Primack J. R., 2004, *ApJ*, 609, 35  
 Mo H.J., Mao S., White S.D.M., 1998, *MNRAS*, 295, 319  
 Lu Y., Mo H. J., Weinberg M. D., Katz N., 2011, *MNRAS*, 416, 1949  
 Lu Y., Mo H. J., Wechsler R. H., 2015, *MNRAS*, 446, 1907  
 McGaugh S. S., 2005, *Phys. Rev. Lett.*, 95, 171302  
 Peebles, P. J. E. 1969, *ApJ*, 155, 393  
 Pizagno J. et al., 2007, *AJ*, 134, 945  
 Reddick R. M., Wechsler R. H., Tinker J. L., Behroozi P. S., 2013, *ApJ*, 771, 30  
 Rodriguez-Gomez V. et al., 2017, *MNRAS*, 467, 3083  
 Sales L. V., Navarro J. F., Schaye J., Dalla Vecchia C., Springel V., Haas M. R., Helmi A., 2009, *MNRAS*, 399, L64  
 Sales L. V. et al., 2012, *MNRAS*, 423, 1544  
 Schaller M. et al., 2015, *MNRAS*, 451, 1247  
 Schaye J. et al., 2015, *MNRAS*, 446, 521  
 Somerville R. S. et al., 2008, *ApJ*, 672, 776-786  
 Somerville R. S. et al., 2017, preprint (arXiv:1701.03526)  
 Springel V., 2005, *MNRAS*, 364, 1105  
 Springel V., White S. D. M., Tormen G., Kauffmann G., 2001, *MNRAS*, 328, 726  
 Stevens A. R. H., Lagos C. d. P., Contreras S., Croton D. J., Padilla N. D., Schaller M., Schaye J., Theuns T., 2016, preprint (arXiv:1608.04389)  
 Teklu A. F., Remus R.-S., Dolag K., Beck, A. M., Burkert A., Schmidt A. S., Schulze F., Steinborn L. K., 2015, *ApJ*, 812, 29  
 Zavala J. et al., 2016, *MNRAS*, 460, 4466  
 Zjupa J., Springel V., 2016, preprint (arXiv:1608.01323)

This paper has been typeset from a  $\text{\LaTeX}$  file prepared by the author.